© 2017. Published by The Company of Biologists Ltd | Development (2017) 144, 3102-3113 doi:10.1242/dev.145854

RESEARCH ARTICLE

The extracellular metalloprotease AdamTS-A anchors neural lineages in place within and preserves the architecture of the central nervous system

James B. Skeath[1,*], Beth A. Wilson[1], Selena E. Romero[1], Mark J. Snee[1], Yi Zhu[1] and Haluk Lacin[2]

ABSTRACT

The extracellular matrix (ECM) regulates cell migration and sculpts organ shape. AdamTS proteins are extracellular metalloproteases known to modify ECM proteins and promote cell migration, but demonstrated roles for AdamTS proteins in regulating CNS structure and ensuring cell lineages remain fixed in place have not been uncovered. Using forward genetic approaches in *Drosophila*, we find that reduction of *AdamTS-A* function induces both the mass exodus of neural lineages out of the CNS and drastic perturbations to CNS structure. Expressed and active in surface glia, *AdamTS-A* acts in parallel to *perlecan* and in opposition to *viking*/*collagen IV* and *βPS-integrin* to keep CNS lineages rooted in place and to preserve the structural integrity of the CNS. *viking*/*collagen IV* and *βPS-integrin* are known to promote tissue stiffness and oppose the function of *perlecan*, which reduces tissue stiffness. Our work supports a model in which AdamTS-A anchors cells in place and preserves CNS architecture by reducing tissue stiffness.

KEY WORDS: AdamTS proteins, Glia, Extra-cellular matrix, Collagen IV, Cell migration

INTRODUCTION

The marriage of form to function is a unifying theme of biology. Yet the genes and pathways that govern tissue architecture remain poorly characterized. The elucidation of these mechanisms is essential for a full understanding of tissue structure, growth and development.

The *Drosophila* CNS adopts its characteristic shape at the end of embryogenesis and maintains this shape through its massive growth during larval stages. In invertebrates and vertebrates, tissue shape is largely dictated by the basement membrane, a special type of extracellular matrix (ECM) that forms a meshed network of protein polymers that surrounds organs, providing them with structural support and resiliency (Yurchenco, 2011). The fly CNS is covered by a thick basement membrane – the neural lamella – that governs CNS structure via its mechanical properties and interactions with underlying glia (Meyer et al., 2014; Stork et al., 2008). The tremendous growth of the CNS during larval stages places great demands on the neural lamella: it must impose structure on the CNS while continually remodeling itself and its interactions with the underlying glia to allow for its own growth and that of the CNS. These properties, together with the power of *Drosophila* genetic, make the fly CNS an ideal system in which to dissect the cellular, genetic and molecular mechanisms that govern tissue architecture and homeostasis during growth and development.

From the outside in, the entire *Drosophila* larval CNS is consecutively enwrapped by the neural lamella, hereafter referred to as the CNS basement membrane, and the membranes of the perineural and subperineural surface glia (Fig. 1); these layers provide structural support to the CNS and insulate it from the hemolymph (Coutinho-Budd and Freeman, 2013). Perineural glia, the outermost cell layer, are small cells that largely arise post-embryonically and divide extensively during larval development to cover the surface of the CNS by the late-third instar stage (Awasaki et al., 2008; Doherty et al., 2009). Perineural glia directly underlie the basement membrane, contribute to the blood-brain barrier (Stork et al., 2008) and help nourish the CNS (Volkenhoff et al., 2015). Sub-perineural glia form an inner-layer of large, polyploid sheet-like cells that associate with each other via septate junctions to form the major component of the fly blood-brain barrier (Bainton et al., 2005; Stork et al., 2008). Internal to these three layers reside thousands of neurons and three other types of glia – cortex, ensheathing and astrocyte-like glia – that enwrap, respectively, the cell bodies, axons and terminal synapses/dendrites of neurons with their cell membranes (Fig. 1) (Awasaki et al., 2008; Doherty et al., 2009). Genetic studies indicate that surface glia control CNS structure: RNAi-mediated depletion of *integrin* function in surface glia yields an elongated nerve cord, suggesting interactions between surface glia and the basement membrane impose structure on the CNS (Meyer et al., 2014). Few other factors, however, have been shown to act in glia to preserve CNS structure.

The major components of basement membranes include Collagen IV, the heparan-sulfate proteoglycan Perlecan [also called *terribly reduced optic lobes* (*trol*) in flies], and Nidogen and Laminin (Fig. 1) (Yurchenco, 2011). These proteins form a multi-layered, meshwork-like covering over most tissues or organs. Tethered to the cell surface largely via interactions between Collagen IV, laminins and cell surface receptors, such as integrins and Dystroglycan, this network provides structure, resiliency and tensile strength to tissues. It also provides a scaffold that helps organize basement membrane assembly and serves as a substrate for cell migration (Yurchenco, 2011). In *Drosophila* imaginal discs, *collagen IV* and *βPS-integrin* appear to promote tissue stiffness or constriction, while *perlecan* appears to act in an opposite manner to reduce tissue stiffness (Kim et al., 2014; Pastor-Pareja and Xu, 2011). The apparent mutual antagonism between these basement membrane proteins likely underlies the semi-rigid, yet resilient, nature of tissues and organs. Additional unidentified factors almost certainly act with these factors to maintain this dynamic homeostasis, essential for the

[1]Department of Genetics, Washington University School of Medicine, 4523 Clayton Avenue, St Louis, MO 63110, USA. [2]Janelia Farm Research Campus, Howard Hughes Medical Institute, 19700 Helix Drive, Ashburn, VA 20147, USA.

*Author for correspondence (jskeath@genetics.wustl.edu)

J.B.S., 0000-0003-1179-4857

Received 16 October 2016; Accepted 21 July 2017

Development (2017) 144, 3102-3113 doi:10.1242/dev.145854

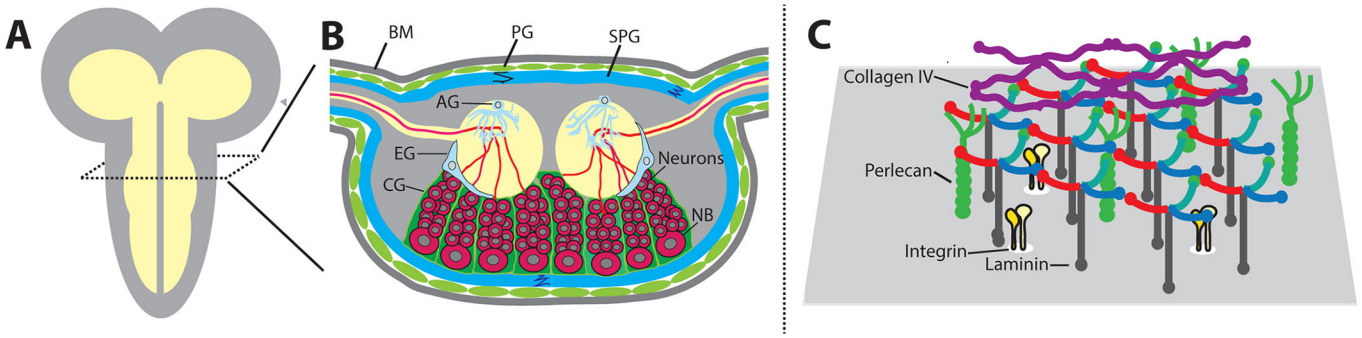

Fig. 1. The *Drosophila* CNS and basement membrane. (A) Overview of the *Drosophila* larval CNS: the cell bodies of neurons and most glia reside in the neuronal cell cortex (gray), whereas axons and synaptic connections occur in the neuropil (yellow). (B) Schematic cross-section of thoracic CNS. The basement membrane (BM), perineural glia (PG) and sub-perineural glia (SPG) fully and consecutively enwrap the entire CNS. Cell bodies of cortex glia (CG) enwrap entire neuronal lineages, including the neuroblast (NB) and neurons. Ensheathing glia (EG) and astrocyte glia (AG) cover the neuropil and send projections within the neuropil to enwrap axons and dendrites. (C) Schematic of major components of the basement membrane – Laminin and Collagen IV – form distinct networks; these networks interact with Perlecan and Integrin cell-surface receptors.

growth and function of basement membranes during larval development.

Genes of the a disintegrin and metalloproteinase with thrombospondin motifs (AdamTS) family encode a large family of extracellular proteases (Kelwick et al., 2015; Kim and Nishiwaki, 2015; Kuno et al., 1997). Different subfamilies of AdamTS proteins preferentially modify different ECM proteins and regulate diverse biological functions (reviewed by Apte, 2009; Rodriguez-Manzaneque et al., 2015). The Gon-1 subfamily of AdamTS proteins, named after *C. elegans gon-1* gene, have been shown to cleave chondroitin sulfate proteoglycans in vertebrates and to promote cell migration in worms and flies (Carlos Rodríguez-Manzaneque et al., 2002; Kelwick et al., 2015; Sandy et al., 2001; Somerville et al., 2003). For example, in *C. elegans*, *gon-1* drives the distal tip cell on its stereotyped 'U'-shaped migration to form the gonad (Blelloch and Kimble, 1999; Nishiwaki et al., 2000). In flies, the ortholog of *gon-1*, *AdamTS-A*, promotes the normal migratory behavior of germ cells, visceral mesoderm, and tracheal cells (Ismat et al., 2013). A role for AdamTS proteins in regulating CNS structure and anchoring cells in place, however, has not been uncovered.

Here, we show that, within *Drosophila*, *AdamTS-A* acts in perineural and sub-perineural surface glia to ensure neural lineages remain fixed in place and to maintain the architectural integrity of the CNS by regulating the organization of the CNS basement membrane and opposing the actions of *viking*/*collagen IV* and *βPS-integrin*. As *collagen IV* and *βPS-integrin* are known to regulate tissue structure by promoting tissue stiffness (Kim et al., 2014; Pastor-Pareja and Xu, 2011), our work supports a model in which AdamTS-A, a molecular scissors, acts to keep cells in place and maintain the architectural integrity of the CNS during its rapid growth in larval stages by relaxing tissues.

RESULTS

The runaway mutation drives a mass exodus of neural lineages from the CNS

In an EMS-based forward genetic screen of over 2000 independently mutagenized third chromosomes, we uncovered a mutation, *runaway*^{1}, that when homozygous led to the exodus of hundreds to thousands of cells out of the CNS through nerves towards and into peripheral tissues, such as eye and leg imaginal discs (Fig. 2A). These invading lineages, often massive in size, are found in the nerves that connect brain lobes to eye discs and the ventral nerve cord to leg discs (Fig. 2A, asterisks), as well as in nerves that connect the nerve cord to other peripheral tissues (Fig. 2B, arrows). The invading cells are composed of neuroblasts (Fig. 2B, arrowhead; Fig. 2C), the stem cells of the CNS and neurons (Fig. 2A-B), indicating that entire neural lineages exit the CNS. This 'neural invasion' phenotype, barely detectable in second instar larvae, becomes fully manifest in third instar larvae (Table 1), concomitant with the most rapid growth phase of the *Drosophila* CNS (Truman and Bate, 1988; Maurange et al., 2008). Despite the size of the invading neural masses, the proliferative index of neuroblasts in *runaway*^{1} larvae appeared similar to wild type (Table S1), indicating the *runaway*^{1} mutation has little effect on cell proliferation. Thus, when homozygous, the *runaway*^{1} lesion severely distorts CNS structure and leads to a mass exodus of neural lineages out of the CNS through nerves to distant tissues.

runaway alleles identify AdamTS-A

During the course of our analysis, we fortuitously uncovered a second non-complementing allele of *runaway*, *runaway*^{2}, tightly linked to the *Sb*^{1} allele (see Materials and Methods). *runaway*^{1} and *runaway*^{2} are recessive alleles that fail to complement each other for the neural invasion phenotype and an associated 2- to 3-day delay in larval development. These alleles thus identify the same gene. To uncover the molecular nature of *runaway*, we used the method of Zhai et al. (2003) to map the *runaway*^{1} developmental delay phenotype to genetic map position 57.4±2.0 (Fig. 3A). Deficiency mapping of this region localized the *runaway*^{1} lesion to a 135 kb genomic region uncovered by *Df(3R)Exel6174* and excluded from *Df(3R)BSC741* and *Df(3R)BSC515* (Fig. 3A). Twenty-four protein-coding genes reside in this region, and both *runaway* alleles failed to complement two alleles of one of these genes – *AdamTS-A* – for the neural invasion and developmental delay phenotypes. Sequence analysis revealed no alterations to the *AdamTS-A* open-reading-frame in either *runaway* allele, but did uncover a Tirant retrotransposon insert in the 5′ most exon of *AdamTS-A* in *runaway*^{1} and a Zam retrotransposon insert in nearly the same location in *runaway*^{2} (Fig. 3B). Using primers that flanked the ~25 kb first intron of *AdamTS-A*, qRT-PCR analysis revealed that the levels of this *AdamTS-A* transcript were reduced to 1.3-3.5% of wild-type levels in the CNS of late-third instar *AdamTS-A*^{rnwy1} larvae (P<0.0005; n=3). We infer that these insertions cause the *runaway* phenotype by reducing the expression and function of the main isoform of *AdamTS-A*, *AdamTS-A[RB]*, which is predicted to

Development (2017) 144, 3102-3113 doi:10.1242/dev.145854

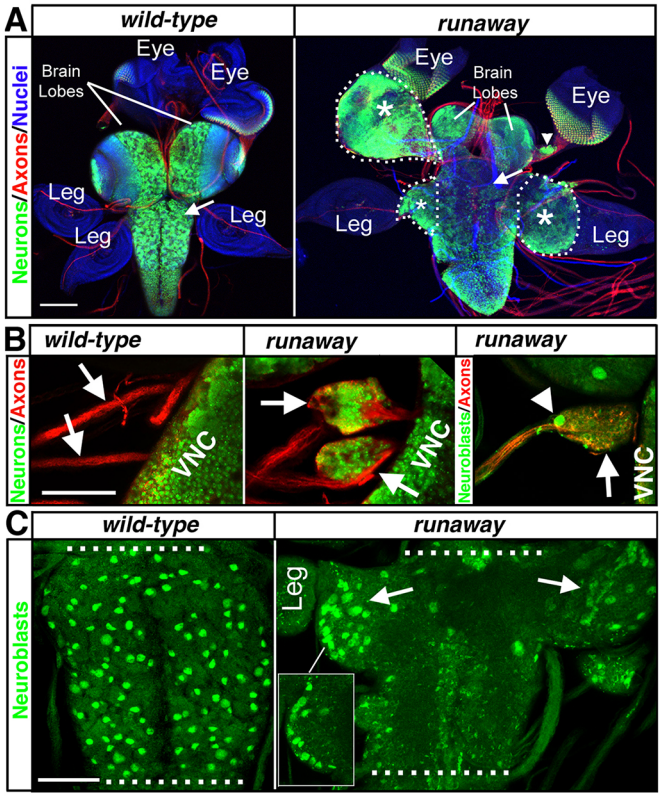

Fig. 2. Mutations in *runaway* lead to the exodus of neural lineages out of the CNS. (A) Ventral views of CNS and imaginal disc complexes of wild-type and *runaway*^{1} mutant late-third instar larvae labeled for ELAV to mark neurons (green), HRP to mark axons (red) and DAPI to label nuclei (blue). Asterisks mark large ectopic neuronal structures, outlined by dotted lines; arrowhead marks small neuronal cluster along the optic stalk; and arrows indicate general loss of neurons (green) from nerve cord in mutant larvae. (B) Ventral views of nerves projecting from the CNS in wild-type and *runaway*^{1} mutant larvae labeled for ELAV or Deadpan (green) and HRP (red); VNC marks the left edge of nerve cord. Arrows indicate nerves in wild type and clusters of neuronal cell bodies within nerves in *runaway* larvae. Arrowhead indicates a Deadpan^{+} neuroblast. (C) Ventral view of neuroblasts (green, arrows) in thoracic neuromeres, marked by dotted lines, in wild-type and *runaway*^{1} mutant late-third instar larvae. Inset shows a single *z*-section. Anterior is upwards (top right for B). Scale bars: 100 µm in A; 50 µm in B,C.

encode a membrane-anchored extracellular protease of an AdamTS subfamily thought to modify and cleave ECM proteins, notably chondroitin sulfate proteoglycans (Carlos Rodríguez-Manzaneque et al., 2002; Kelwick et al., 2015; Sandy et al., 2001; Somerville et al., 2003). We now refer to the *runaway* alleles as *AdamTS-A*^{rnwy1}

Table 1. Time course analysis of the *runaway* CNS phenotype

	Morphology of the CNS		
Stage*	Wild type	Mild bulging of the CNS	Overt neural invasion
24 h ALH	90% (*n*=18/20)	10% (*n*=2/20)	0% (*n*=0/20)
48 h ALH	82.4% (*n*=13/17)	17.6% (*n*=3/17)	0% (*n*=0/17)
72 h ALH	35.1% (*n*=13/37)	43.2% (*n*=16/37)	21.6% (*n*=8/37)
6 h AL3E	0% (*n*=0/15)	33.3% (*n*=5/15)	66.7% (*n*=10/15)
24 h AL3E	7.7% (*n*=1/13)	7.7% (*n*=1/13)	84.6% (*n*=11/13)
48 h AL3E	0% (*n*=0/12)	8.3% (*n*=1/12)	91.7% (*n*=11/12)
72 h AL3E	0% (*n*=0/15)	0% (*n*=0/15)	100% (*n*=15/15)

n=the number of larvae scored.
*All stages are ±6 h.
ALH, after larval hatching; AL3E, after third instar ecdysis.

and *AdamTS-A*^{rnwy2}. As cellular stress is known to enhance retrotransposon jumping in many eukaryotes (Capy et al., 2000), we speculate that our EMS treatment enhanced retrotransposon jumping by inducing cellular stress, leading to the insert of the Tirant element in *AdamTS-A* in *runaway*^{1}.

Despite the severity of the neural invasion phenotype, genetic tests identify both alleles as hypomorphic (Table 2). Flies homozygous for *AdamTS-A*^{rnwy1} or trans-heterozygous for *AdamTS-A*^{rnwy1} and *AdamTS-A*^{rnwy2} eclosed as uncoordinated, sub-fertile adults at ∼60% the expected frequency of wild type (Table 2). In contrast, flies transheterozygous for the *AdamTS-A*^{KO} null allele and *Df(3R)88F5*, a small deficiency of the region (Ismat et al., 2013), are lethal at the second larval instar (Table 2) and exhibit a CNS reduced in size with rare instances of perturbed structure and neural invasion (Fig. 3Cv, arrowhead). Flies transheterozygous for either *AdamTS-A*^{rnwy1} or *AdamTS-A*^{rnwy2} and *AdamTS-A*^{KO} or *Df(3R)88F5* rarely pupated and eclosed (Table 2). Larvae of these genotypes that reach the late-third larval instar stage exhibit a severe neural invasion phenotype (Fig. 3Ciii), whereas those that fail to reach this stage exhibit a milder neural invasion phenotype, likely due to an earlier block in development [Fig. 3Civ; compare size of leg discs (dotted lines) between Fig. 3Ciii,Civ]. Thus, the *runaway* phenotype appears to manifest in conditions of reduced, but not abrogated, *AdamTS-A* function.

AdamTS-A acts in glia to preserve CNS structure and anchor cells in place

The CNS is composed primarily of neurons and glia. To determine whether the genetic function of *AdamTS-A* is required in neurons or glia, or both, to regulate CNS architecture and keeps cells in place, we used the GAL4/UAS system to deplete *AdamTS-A* function via RNAi in either all neurons or all glia of otherwise wild-type larvae (Brand and Perrimon, 1993) (see Materials and Methods). When *AdamTS-A* function was depleted specifically in neurons (*elav>AdamTS-A*^{RNAi}*; repoGAL80*), no larvae exhibited a neural invasion phenotype (*n*=34; Fig. 4Aiii). In contrast, when *AdamTS-A* function was depleted specifically in glia (*repo>AdamTS-A*^{RNAi}), 48 out of 49 larvae exhibited a strong neural invasion phenotype (Fig. 4Aii). Thus, the genetic function of *AdamTS-A* is required in glia to maintain CNS structure and ensure neural lineages stay put.

To see whether *AdamTS-A* expression is sufficient to rescue the *AdamTS-A*^{rnwy} phenotype, we drove its expression in all neurons or all glia of otherwise *AdamTS-A*^{rnwy} mutant larvae. Here, we used UAS-linked transgenes for *AdamTS-A[RB]* as well as *AdamTS-A [RE]* (Ismat et al., 2013), which encodes the smallest *AdamTS-A* isoform; the encoded proteins are essentially identical, except that AdamTS-PE lacks a membrane anchor. Both transgenes behaved identically in the assays. Expression of *AdamTS-A* in neurons failed to rescue the neural invasion phenotype of *AdamTS-A*^{rnwy} mutant larvae ($n \geq 13/13$; Fig. 4Biii) and had no discernible effect on CNS morphology of wild-type larvae ($n \geq 20/20$; Fig. 4Ciii). In contrast, expression of *AdamTS-A* in glia fully rescued the *AdamTS-A*^{rnwy} neural invasion phenotype and replaced it with one marked by an elongated nerve cord and flattened brain lobes ($n \geq 15/15$; Fig. 4Bii), a phenotype identical to that observed upon glial overexpression of *AdamTS-A* in wild-type larvae ($n \geq 30/30$; Fig. 4Cii). Thus, *AdamTS-A* expression in glia is sufficient to rescue the *AdamTS-A*^{rnwy} phenotype and the ability of *AdamTS-A* overexpression in glia to elongate the nerve cord and deflate brain lobes suggests *AdamTS-A* controls CNS structure by relaxing the tissue. We note that the level of *AdamTS-A* expression is a key determinant of phenotype:

Development (2017) 144, 3102-3113 doi:10.1242/dev.145854

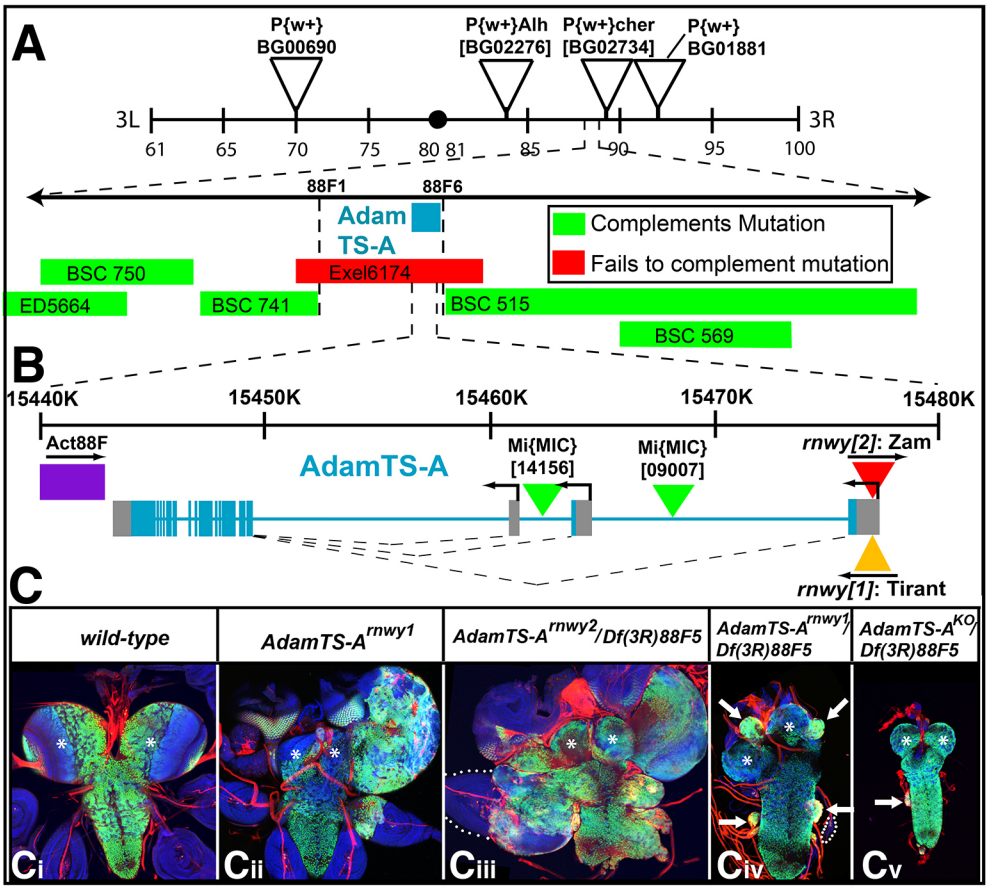

Fig. 3. *runaway* alleles identify *AdamTS-A*. (A) The developmental delay and neural invasion phenotypes of *runaway*^{1} and *runaway*^{2} were localized to genomic region 88F via meiotic mapping with P elements and deficiency mapping with molecularly defined deficiencies. (B) The *AdamTS-A* genomic locus with sites of the *AdamTS-A*^{rnwy1} (Tirant: 3R-15476078) and *AdamTS-A*^{rnwy2} (Zam: 3R-15476080) lesions indicated (Genome version R6.15). (C) Ventral views of photomontages of brain-nerve cord complexes and associated imaginal discs from third instar larvae of indicated genotypes labeled for neurons (ELAV, green), axons (HRP, red) and nuclei (DAPI, blue). Asterisks mark the brain. In, iii and iv, dotted lines outline leg discs; in iv and v, arrows indicate examples of neural invasion.

low level expression of *AdamTS-A* in glia, as occurs when *AdamTS-A* is expressed under the control of the neural-specific *elavGAL4* driver in the absence of *repoGAL80* (Berger et al., 2007), is sufficient to restore *AdamTS-A*^{rnwy} mutant nerve cords to wild-type morphology (Fig. 4Biv).

To determine whether the proteolytic activity of AdamTS-A is essential for its rescuing activity, we repeated the above experiments with protease-dead versions of *AdamTS-A* – *AdamTS-A*^{E591A} for *AdamTS-A[RB]* and *AdamTS-A*^{E439A} for *AdamTS-A[RE]*, both of which behaved identically in the assays. In the zinc-binding metalloproteases of which AdamTS-A is a member, this E-to-A mutation (underlined) in the consensus catalytic protease site (HEXXHXXG/N/SXXHD) reduces enzymatic activity ~1900-fold without altering protein structure or stability (Crabbe et al., 1994). As observed above, expression of the protease-dead versions of *AdamTS-A* in neurons failed to rescue the *AdamTS-A*^{rnwy} neural invasion phenotype and had no gross effect on CNS morphology in wild-type larvae (not shown). In contrast, expression of the transgenes in glia of wild-type larvae led to an elongated nerve cord ($n \geq 11/11$; Fig. 4Civ), a phenotype similar to but less severe than that observed upon overexpression of wild-type *AdamTS-A* in glia (compare Fig. 4Cii with Civ). Expression of the transgenes in glia of *AdamTS-A*^{rnwy} larvae partially rescued the neural invasion phenotype: ~45% of larvae exhibited a modest neural invasion phenotype and an elongated nerve cord (n=14/31; Fig. 4Bvi), and ~55% of larvae lacked a neural invasion phenotype and exhibited an elongated nerve cord (n=17/31; Fig. 4Bv). The observation that protease-dead forms of *AdamTS-A* provide significant, yet partial, rescuing activity suggests *AdamTS-A* preserves CNS structure and keeps cells in place through protease-dependent and -independent mechanisms. Owing to our inability to generate high-quality AdamTS-A antibodies, we could not determine whether the wild-type and protease-dead *AdamTS-A* transgenes drove protein expression at similar levels. Thus, it remains formally possible that some of the phenotypic differences observed between expression of the wild-type and protease-dead *AdamTS-A* transgenes may arise due to differences in protein expression.

Table 2. Survival of different *AdamTS-A* allelic combinations

	Stage of development	
Genotype	Pupal	Adult
AdamTS-A^{rnwy1}/*AdamTS-A*^{rnwy1}	85.2±47.4%	60.6±37.5%
AdamTS-A^{rnwy1}/*AdamTS-A*^{rnwy2}	84.1±34.4%	56.6±38.1%
AdamTS-A^{rnwy1}/*Df(3R)88F5*	0.4+1.1%	0.4+1.1%
AdamTS-A^{rnwy2}/*Df(3R)88F5*	14.4+6.9%	3.7+3.7%
AdamTS-A^{rnwy1}/ *AdamTS-A*^{KO}	0	0
AdamTS-A^{rnwy2}/*AdamTS-A*^{KO}	5.4+10.3%	0
Df(3R)88F5/ *AdamTS-A*^{KO}	0	0

Values indicate the percentage of flies of the indicated genotype that reached noted stage based on observed number of *mutant*/*TM6 Tb* progeny from a *mutant[1]*/*TM6* Tb×*mutant[2]*/*TM6 Tb* cross. For each genotype, n>6 trials and n>200 progeny.

AdamTS-A is expressed and functions in perineural and sub-perineural glia

At least five different subtypes of glia reside within the CNS (Coutinho-Budd and Freeman, 2013). To pinpoint whether *AdamTS-A* acts within all or a defined subset of these glia, we generated a transcriptional reporter of the *AdamTS-A[RB]* transcript from the Mi{MIC}[09007] insert (*AdamTS-A*^{GAL4}; Fig. 2B; see

Development (2017) 144, 3102-3113 doi:10.1242/dev.145854

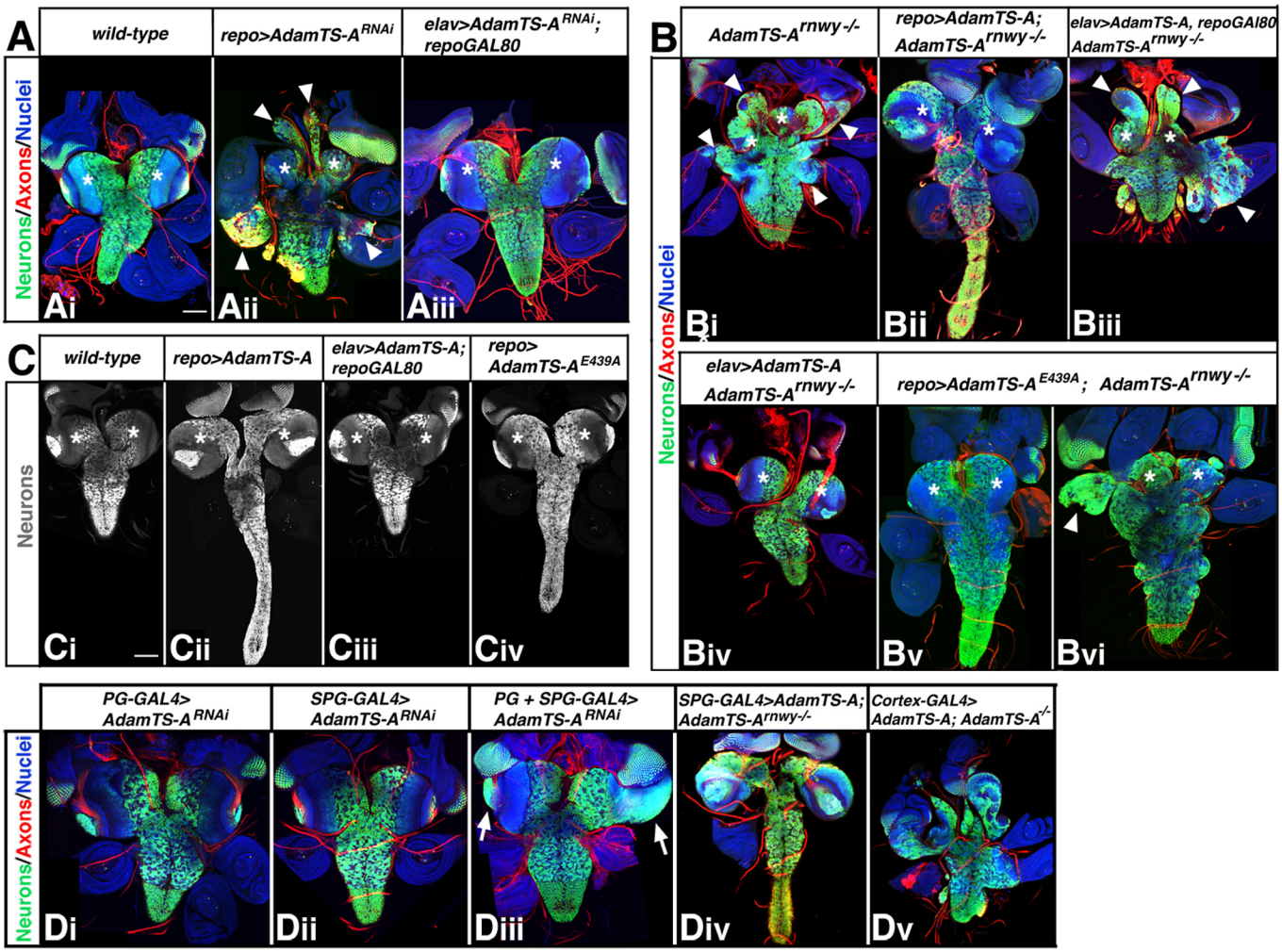

Fig. 4. Reduction of *AdamTS-A* function in glia trigger the neural invasion phenotype. (A) Ventral views of photomontages of CNS and imaginal disc complexes from late-third instar larvae of indicated genotypes labeled for neurons (ELAV, green), axons (HRP, red) and nuclei (DAPI, blue). Asterisks indicate brain lobes; arrowheads indicate instances of neural invasion. (B) Ventral views of photomontages of CNS and imaginal disc tissue from late-third instar larvae of indicated genotypes labeled as in A. Asterisks indicate brain lobes; arrowheads indicate instances of neural invasion. (C) Ventral views of photomontages of the CNS of late-third instar larvae of indicated genotype labeled for ELAV to mark neurons (grayscale). Asterisks indicate brain lobes. (D) Ventral views of photomontages of CNS and imaginal disc tissue from late-third instar larvae of indicated genotypes labeled as in A. Arrows indicate instances of neural invasion. In A, wild type is *UAS-AdamTS-A^{WT}/+*. In B, *AdamTS-A$^{-/-}$* is *AdamTS-A^{rnwy1}/AdamTS-A^{rnwy2}*. In C, wild type is *UAS-AdamTS-A^{RNAi}/+; UAS-DCR2/+*. Anterior is upwards. Scale bar: 100 µm. For more details of the full genotypes, see the supplementary Materials and Methods.

Materials and Methods) and used it to drive a nuclear-targeted GFP transgene in *AdamTS-A*-expressing cells (Fig. 5). Within the CNS, this reporter specifically labeled all perineural and sub-perineural glia (Fig. 5Ai; Fig. S1), which completely and consecutively enwrap the entire surface of the CNS, but did not appear to label cortex or astrocyte-like glia, which are found internally in the CNS, or neurons (Fig. 5Aii-iv; Fig. S1). Owing to the sparse nature of ensheathing glia and their co-mingling with perineural and sub-perineural glia, we cannot exclude that some ensheathing glia also express *AdamTS-A*. Within perineural and subperineural glia, *AdamTS^{GAL4}* activates gene expression during the second larval instar stage, coincident with when the *AdamTS-A* neural invasion phenotype first starts to manifest (not shown; Table 1). Identical results were obtained from a second *AdamTS-A* GAL4 transcriptional reporter generated from the Mi{MIC}[14156] insert (Fig. 3B; Fig. S2). And, RNA *in situ* analysis of *AdamTS-A* transcript confirmed that these transcriptional reporters faithfully recapitulated endogenous *AdamTS-A* expression (Fig. S2).

To test whether *AdamTS-A* function is required in either perineural or sub-perineural glial cells, or both, to preserve CNS architecture, we depleted *AdamTS-A* function in either cell type of both cell types via RNAi. Depletion of *AdamTS-A* function in either perineural glia (*PG-GAL4*) or sub-perineural glia (*SPG-GAL4*) failed to elicit a neural invasion phenotype (n>0/15 larvae per genotype; Fig. 4Di,Dii), but depletion of *AdamTS-A* function in both glial subtypes yielded a mild neural invasion phenotype ~90% of the time (n=21/23; Fig. 4Diii). We infer that *AdamTS-A* acts in both perineural and subperineural glia to anchor neural lineages and preserve CNS structure. Consistent with this model, *AdamTS-A* expression in subperineural glia, but not cortex glia, was sufficient to rescue the *AdamTS-A* neural invasion phenotype (Fig. 4Div,Dv), although *AdamTS-A* expression in perineural glia resulted in embryonic or early larval lethality.

In *AdamTS-A^{rnwy}* larvae, perineural and sub-perineural glia form, survive and completely enwrap the CNS, including the invading neural masses that are minimally composed of neurons, neuroblasts

Development (2017) 144, 3102-3113 doi:10.1242/dev.145854

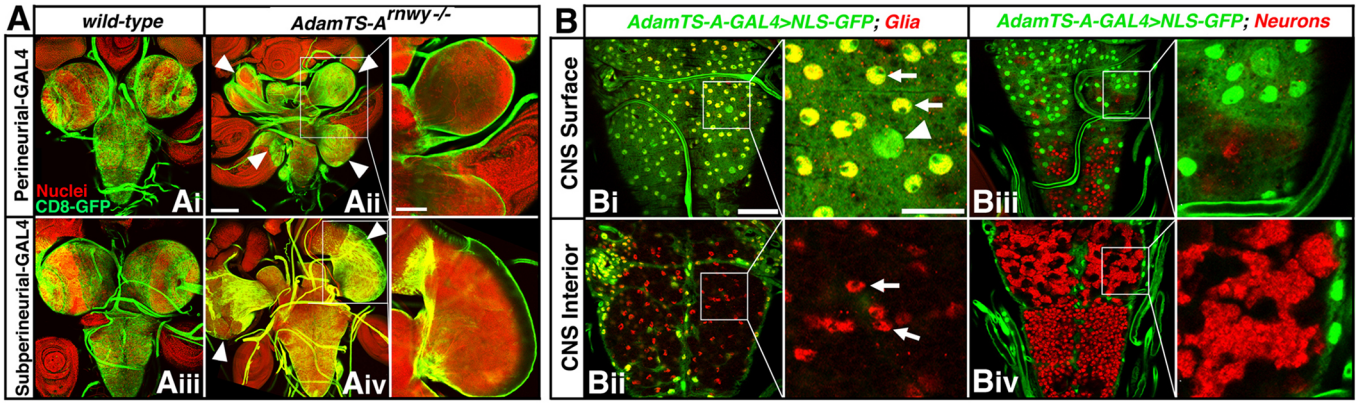

Fig. 5. *AdamTS-A* is expressed in perineural and subperineural glia. (A) Ventral views of tiled images of the CNS of late third instar wild-type (Ai, Aiii) or *AdamTS-A*^{rnwy} mutant larvae (Aii, Aiv) labeled for nuclei (red) and the membranes (green) of perineural glia or subperineural glia. Arrowheads mark ectopic neural structures (Aii, Aiv), which are encased within the membranes of perineural and subperineural glia (insets). Scale bar: 100 µm in Ai-Aiv; 50 µm for enlargements. (B) Ventral views of nerve cords from late third instar *AdamTS-A*$_{GAL4}$*>UAS-NLS-GFP* larvae labeled using Repo antibodies to label glia (red, Bi,ii) or with ELAV antibodies to label neurons (red, Biii,iv) and GFP (green; Bi-iv). In the enlargement of Bi, arrows indicate perineural glia and the arrowhead indicates sub-perineural glia. In the enlargement of Bii, arrows indicate cortex glia. Scale bar: 50 µm for Bi-iv; 20 µm for enlargements. For more details of the full genotypes, see the supplementary Materials and Methods.

and cortex glia (Fig. 5B; Fig. S3). All other glial subtypes also form, survive and differentiate (Fig. S3). Thus, the neural lineages and cortex glia that inappropriately exit the CNS in *AdamTS-A*^{rnwy} mutant larvae typically do not break through any glial cell layers in the CNS or the basement membrane. Rather, they tunnel through the nerves out of the CNS toward peripheral tissues, fully encased by the surface glia the entire time (Fig. 5B; Fig. S3). As surface glia appear to be the only cells that express *AdamTS-A* in the CNS, reduction of *AdamTS-A* function in these two cell types may trigger, apparently in a non-autonomous manner, the underlying neural lineages and cortex glia to exit the CNS.

AdamTS-A and *perlecan* yield similar CNS phenotypes

Basement membranes regulate tissue structure and cell migration, the two key processes disrupted in the CNS upon reduction of *AdamTS-A* function. In flies, the CNS basement membrane directly overlies the surface glia, and mammalian orthologs of AdamTS-A are known to associate with and cleave basement membrane proteins (Apte, 2009; Sandy et al., 2001). Thus, we first asked whether reduction in the function of three key basement membrane constituents – laminins, Perlecan and Viking (one of two type IV collagens in flies) – and a main cellular receptor for laminins and Collagen IV, βPS-Integrin (*myospheroid*), yielded phenotypes similar to those observed for *AdamTS-A*. Reduction of *laminin A* or *laminin B* function during larval stages did not grossly disrupt CNS morphology (not shown), but reduction of function in *perlecan* [originally identified as *terribly reduced optic lobes* (*trol*)] led to CNS phenotypes similar to those of *AdamTS-A*^{rnwy} mutant larvae (Fig. 6A-B): the presence of ectopic neural masses in the optic stalk and protrusions of varied size from the brain and nerve cord. These phenotypes were highly penetrant in larvae depleted for *trol* function via RNAi (n=21/22) and in *trol*^{G0271} hypomorphic mutant larvae (n=20/21) (Fig. 6A,B), where larvae reached the third-larval instar stage, but were less penetrant in larvae mutant for stronger *trol* alleles, such as *trol*^{8} (n=8/22) and *trol*^{SD} (n=1/5), which typically arrest in the second-larval instar stage (Fig. S4; not shown).

To explore the functional relationship between *AdamTS-A* and *perlecan*, we asked whether overexpression of each gene modified the loss of function phenotype of the other. We found that *AdamTS-A* overexpression in glia in *trol*^{G0271} (n=25/25) or *trol*^{SD} (n=10/10) mutant larvae gave rise to an elongated nerve cord (Fig. 6D; Fig. S4). Thus, *perlecan* is not required for AdamTS-A to exerts its effects on CNS structure. *AdamTS-A* overexpression, however, did not suppress *perlecan*-dependent growth defects, as *trol*^{SD} mutant larvae remained arrested in the second larval-instar stage even when *AdamTS-A* was overexpressed (Fig. S4). Similarly, *perlecan* overexpression in the fat body, a center of basement membrane protein synthesis (Pastor-Pareja and Xu, 2011), suppressed the *AdamTS-A* neural invasion phenotype (Fig. 6C, Table 3), even though *perlecan* overexpression on its own had no gross effect on CNS structure. Thus, *perlecan* can modify CNS structure when *AdamTS-A* function is limiting. We infer that *AdamTS-A* and *perlecan* act in parallel to regulate CNS structure and anchor cells in place.

AdamTS-A acts in opposition to Collagen IV and βPS-Integrin to regulate CNS structure

In contrast to *perlecan*, knockdown of *viking* function or glial-specific knockdown of *βPS-integrin* function yielded a phenotype similar to that observed upon overexpression of *AdamTS-A* in glia (Fig. 6H) – an elongated ventral nerve cord (Fig. 6F,G). The similarity of the phenotypes suggests *AdamTS-A* acts opposite *viking* and *βPS-integrin* to regulate CNS structure. If *viking* and *β-integrin* oppose *AdamTS-A* function during CNS development, reduction of their function should suppress the *AdamTS-A*^{rnwy} neural invasion phenotype. In support of this model, a small deficiency, *Df(2L) BSC172*, that removes *viking* and the other type IV collagen gene in *Drosophila* dominantly suppressed the *AdamTS-A*^{rnwy} neural invasion phenotype (Table 3). More impressively, knockdown of *viking* function or glial-specific knockdown of *β-integrin* function strongly suppressed the *AdamTS-A*^{rnwy} neural invasion phenotype (Table 3, Fig. 6I-K). Confirming the specificity of these interactions, mutations in *laminin A*, *laminin B* or three other ECM or cell adhesion molecules failed to reproducibly suppress the *AdamTS-A* neural invasion phenotype (Table 3), and RNAi-mediated depletion of *laminin A*, *laminin B*, *ras* or *raf* function also failed to suppress the *AdamTS-A* neural invasion phenotype (Table 3). We infer that the neural invasion phenotype observed in *AdamTS-A*^{rnwy} larvae requires *collagen IV* and *βPS-integrin* function, and that *AdamTS-A* normally

Development (2017) 144, 3102-3113 doi:10.1242/dev.145854

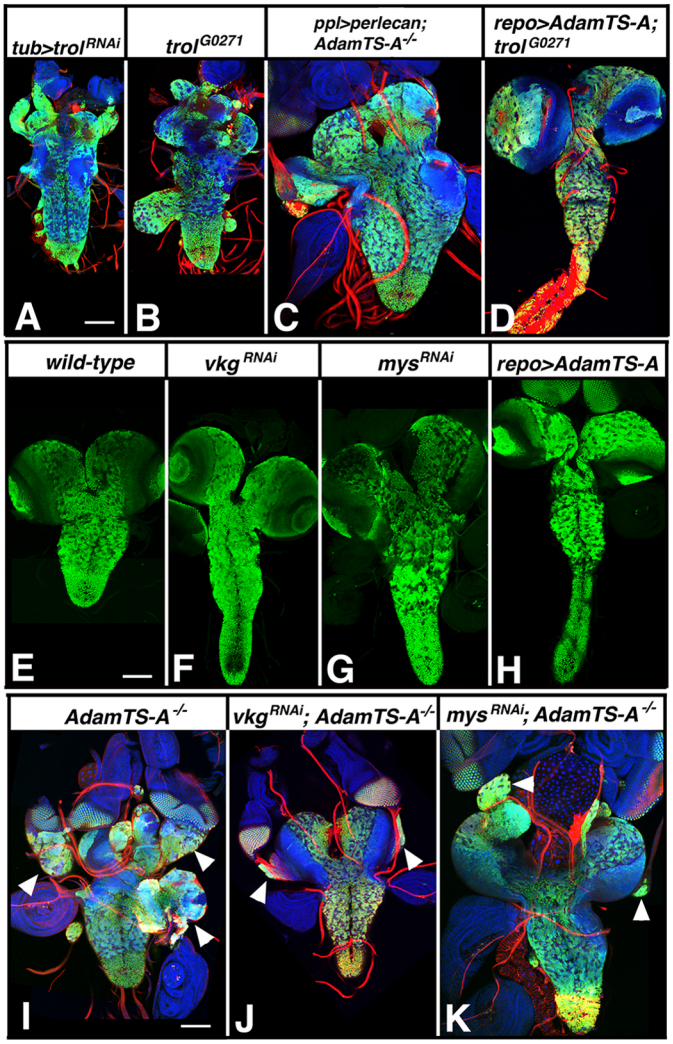

Fig. 6. Reduction of *viking* or *integrin* function suppresses the *runaway* phenotype. (A-K) Ventral views of tiled images of brain-nerve cord complexes from late-third instar larvae of the indicated genotypes labeled for (A-D,I-K) neurons (ELAV, green), axons (HRP, red) and nuclei (DAPI, blue), or (E-H) neurons (green). Arrowheads indicate instances of neural structures or overt deformations in CNS structure. Anterior is upwards. Scale bars: 100 µm.

opposes the action of *viking*/*collagen IV* and *βPS-integrin* to preserve CNS structure and anchor neural lineages in place.

AdamTS-A inhibits accumulation of Collagen IV on the CNS basement membrane

The opposing actions of *AdamTS-A* and *viking/collagen IV* led us to examine the effect of reducing or increasing *AdamTS-A* function on the distribution of Viking, as well as Perlecan and Laminin in the CNS basement membrane using antibodies specific to Perlecan and Laminin (Fessler et al., 1987; Friedrich et al., 2000) and a Viking-GFP protein trap (Morin et al., 2001). In wild type, Viking-GFP, Perlecan and Laminin display a smooth, uniform laminar-like localization along the surface of the brain lobes and ventral nerve cord (Fig. 7A,C; Fig. S5). In *AdamTS-A^{rnwy}* mutant larvae, these proteins accumulate on the surface of the CNS, but are also found in irregularly shaped puncta or aggregates at or near the surface of perineural glia (Fig. 7B,D; Fig. S5). Western blot assays confirmed increased Viking-GFP levels in *AdamTS-A^{rnwy}* larvae relative to wild type (Fig. 7H). Of note, we observe these puncta of ECM material in all *AdamTS-A^{rnwy}* backgrounds, including those in which we deplete *viking* and *βPS-integrin* function. This phenotype is then independent of the *AdamTS-A* neural invasion phenotype, but appears tightly linked to reduction of *AdamTS-A* function.

In support of the model that *AdamTS-A* inhibits the accumulation of Viking-GFP/Collagen IV in the CNS basement membrane, overexpression of *AdamTS-A* triggered a strong decrease in Viking-GFP accumulation in the CNS basement membrane (Fig. 7E-G). This phenotype was accompanied by increased Perlecan levels but not Laminin levels (Fig. 7E-G). Western blot assays confirmed decreased Viking-GFP levels in the CNS basement membrane upon *AdamTS-A* overexpression (Fig. 7H). We infer that *AdamTS-A* opposes tissue stiffness at least in part by opposing Viking/Collagen IV accumulation in the CNS basement membrane.

DISCUSSION

Our work, coupled with the molecular nature of *AdamTS-A* and the tissue organizing role of the basement membrane, indicate that *AdamTS-A* acts in surface glia to preserve CNS structure and keep neural lineages in place by opposing the actions of *collagen IV/viking* and *βPS-integrin*. In this role, our work suggests *AdamTS-A* acts in parallel to *perlecan*, which yields a similar CNS phenotype to *AdamTS-A*, and has been shown to function opposite *collagen IV/viking* to inhibit tissue stiffness in imaginal discs (Pastor-Pareja and Xu, 2011). These findings point to a finely tuned balance between the actions of *AdamTS-A* and *perlecan*, and those of *collagen IV* and *βPS-integrin*, being crucial for homeostatic control of CNS structure. On one side of the balance, *collagen IV/viking* and *βPS-integrin* function to promote tissue or matrix stiffness; on the other side, *AdamTS-A* and *perlecan* function to oppose the actions of *collagen IV/viking* and *βPS-integrin*, and thus inhibit tissue or matrix stiffness. Imbalance in either direction triggers gross defects in CNS structure: flattened brain lobes and an elongated nerve cord when the balance tilts towards *AdamTS-A* and *perlecan*, and gross structural defects and neural invasion when the balance tilts toward *collagen IV/viking* and *βPS-integrin*. Thus, opposing, yet balanced, molecular forces appear to help bestow on the CNS basement membrane its unique combination of stiffness, compliance and resiliency that is essential for preservation of CNS structure during its rapid growth in larval stages.

What molecular pathways drive the runaway neural invasion phenotype?

Reduction of *AdamTS-A* function triggers the mass exodus of scores of neuronal lineages and cortex glia out of the CNS through nerves towards and onto peripheral tissues, such as eye and leg imaginal discs. Throughout their journey, the invading cells appear fully encased by surface glia and the basement membrane and thus likely tunnel through nerves toward these peripheral tissues. As *AdamTS-A* appears to be expressed and function in surface glia, but not in neurons or cortex glia – the cells that actually invade the nerves – our data raise the intriguing possibility that *AdamTS-A* acts non-autonomously to drive the exodus of neural lineages from the CNS.

How might loss of *AdamTS-A* in surface glia trigger the apparent migration of neuronal lineages and cortex glia out of the CNS? We find that *collagen IV/Viking* and *βS-integrin* function are required for the neural invasion phenotype observed in *AdamTS-A^{rnwy}* mutant larvae and that *AdamTS-A* negatively regulates Collagen IV/Viking levels on the CNS basement membrane. In addition and as noted, *viking* and *βPS-integrin* have been shown to promote tissue stiffness or tension in *Drosophila* (Kim et al., 2014; Pastor-Pareja and Xu, 2011), and work from vertebrate systems reveals that

Development (2017) 144, 3102-3113 doi:10.1242/dev.145854

Table 3. Genetic suppression of *AdamTS-A^{rnwy}* phenotype

Genotype	Neural invasion into eye or leg discs*	Number of larvae	Significance level
Wild type	0% (*n*>0/100)	>30	-
AdamTS-A^{rnwy1}	93.5% (*n*=86/92)	23	-
AdamTS-A$^{rnwy1/2}$	87.0% (*n*=107/123)	35	-
laminin$A^{MI06740}$ AdamTS-A$^{rnwy1/2}$	46.7% (*n*=86/184)	49	*P*<0.0001‡,§
laminin$A^{MI02491}$; AdamTS-A$^{rnwy1/2}$	85.7% (*n*=84/98)	37	N/S
laminin$B^{KG03456}$/+; AdamTS-A^{rnwy1}	90.2% (*n*=46/51)	13	N/S
Dg^{B48}/+; AdamTS-A$^{rnwy1/2}$	97.9% (*n*=46/47)	13	N/S
Df(2 L)BSC172/+; AdamTS-A^{rnwy1}	71.6% (*n*=73/102)	26	*P*<0.01‡,¶
shg^{R69}/+; AdamTS-A^{rnwy1}	100% (*n*=20/20)	6	N/S
sdc^{K10215}/+; AdamTS-A^{rnwy1}	92.7% (*n*=38/41)	11	N/S
repoGAL4, AdamTS-A$^{rnwy1/2}$	88.7% (*n*=63/71)	21	-
repo>mys^{RNAi} AdamTS-A$^{rnwy1/2}$	24.6% (*n*=16/65)	17	*P*<1×10^{-8}‡,**
repo>mys^{RNAi} AdamTS-A$^{rnwy1/2}$	30.0% (*n*=15/50)	13	*P*<1×10^{-8}‡,**
repoGAL80, elav>mys^{RNAi} AdamTS-A$^{rnwy1/2}$	87.9% (*n*=58/66)	19	N/S‡,**
TubGAl80^{TS}/+; TubGAL4 AdamTS-A$^{rnwy1/2}$	86.6% (*n*=97/112)	28	-
TubGAl80^{TS}/+; TubGAL4>vkg^{RNAi} AdamTS-A$^{rnwy1/2}$	20.5% (*n*=23/112)	28	*P*<1×10^{-10}‡,‡‡
TubGAl80^{TS}/+; TubGAL4> LanA^{RNAi} AdamTS-A$^{rnwy1/2}$	85.0% (*n*=85/100)	25	N/S‡,‡‡
TubGAl80^{TS}/+; TubGAL4> LanB1^{RNAi} AdamTS-A$^{rnwy1/2}$	82.2% (*n*=88/107)	29	N/S‡,‡‡
pplGAL4, AdamTS-A$^{rnwy1/2}$	90.9% (*n*=100/110)	28	
pplGAL4>UAS-perlecan, AdamTS-A$^{rnwy1/2}$	60.6% (*n*=77/127)	31	*P*<0.0001‡,§§
repo>ras^{DN}, AdamTS-A$^{rnwy1/2}$	88.9% (*n*=40/45)	13	N/S
repo>raf^{DN}, AdamTS-A$^{rnwy1/2}$	100% (*n*=32/32)	9	N/S

*Larvae were scored on each bilateral side for the presence of clusters of neurons in the nerves that innervate the eye and leg imaginal discs. Larvae with neurons in the nerves projecting into eyes and legs on each bilateral side were given a score of 4 out of 4.
N/S, not significant.
‡Fisher's exact test.
§Relative to *AdamTS-A$^{rnwy1/2}$*.
¶Relative to *AdamTS-A^{rnwy1}*.
**Relative to *repoGAL4, AdamTS-A$^{rnwy1/2}$* or *repoGAL80, elav>mys^{RNAi} AdamTS-A$^{rnwy1/2}$*.
‡‡Relative *to TubGAl80^{TS}/+; TubGAL4 AdamTS-A$^{rnwy1/2}$*.
§§Relative to *pplGAL4, AdamTS-A$^{rnwy1/2}$*.

increased tissue or matrix stiffness can induce cell migration and cancer metastasis (Kai et al., 2016; Lo et al., 2000), likely at least in part by activating Rho-Actin signaling and the SRF pathway (Medjkane et al., 2009). Thus, reduction of *AdamTS-A* function in surface glia may allow for increased *collagen IV/viking* and *βPS-integrin* function and a resulting increase in tissue or matrix stiffness, which could trigger Rho-Actin signaling and the SRF pathway to drive cell migration. Alternatively, reduction of *AdamTS-A* function, and its apparent ability to relax tissue stiffness, may inhibit the ability of the CNS basement membrane to breathe and expand as the CNS grows rapidly during the third larval instar stage, leading to a compressive stress that causes groups of neural lineages to become passively squeezed out of the CNS through nerves. Clearly, future work that tests the effect of *AdamTS-A* on matrix stiffness and the role of Rho-Actin signaling and the SRF pathway in promoting the neural invasion phenotype will help clarify the molecular basis through which *AdamTS-A* anchors cells in place in the *Drosophila* CNS.

Does AdamTS-A act through protease-dependent and -independent mechanisms?

Our work raises the possibility that *AdamTS-A* preserves CNS structure and anchors cells in place through proteolytic-dependent and -independent activities, as protease-dead versions of AdamTS-A appear to provide partial, yet significant, rescuing activity. In flies, current substrates of AdamTS-A remain largely unknown. Our work, however, identifies Collagen IV/Viking as a potential substrate: Viking levels in the CNS are increased in *AdamTS-A^{rnwy}* loss-of-function mutants and decreased upon *AdamTS-A* overexpression in glia. Clearly, it will be important to see whether Viking is a substrate of AdamTS-A and to identify additional AdamTS-A substrates and interacting proteins. In this context, we note that the most closely related mammalian homologs of *AdamTS-A* have been found to cleave chondroitin-sulfate proteoglycans (CSPGs) rather than Collagen IV (Somerville et al., 2003), ECM molecules known to repress axon guidance and regeneration and neural cell migration (Burnside and Bradbury, 2014; Zimmer et al., 2010). In flies, AdamTS-A may then also act through CSPGS to govern CNS structure and cell movement. Clearly, directed proteomic and biochemical studies are required to identify AdamTS-A substrates and interacting proteins and to clarify the precise molecular basis through which *AdamTS-A* preserves CNS structures and keeps neural lineages rooted in place.

CNS structure defects manifest upon reduction, not ablation, of *AdamTS-A* and *perlecan* function

Why does reduction, but not elimination, of *AdamTS-A* or *perlecan* function disrupt CNS structure and trigger neural invasion? Elimination of *AdamTS-A* or *perlecan* activity blocks larval development in the first or second larval instar stage, yielding a small, but largely morphologically normal, CNS (Datta, 1995; Datta and Kankel, 1992; this paper). Prior work indicates that *perlecan* function is required to reactivate neuroblast proliferation and promote CNS growth during larval stages (Datta, 1995). The small size of the CNS of larvae homozygous for null alleles of *AdamTS-A* suggest it too is required for larval neuroblast reactivation and CNS growth during larval stages. In contrast, reduction of *AdamTS-A* or *perlecan* function allows for continued neurogenesis and CNS growth during larval life and also triggers the neural invasion phenotype and the gross distortion of CNS structure. CNS growth may then be a pre-requisite for these phenotypes to manifest, as only in the presence of CNS growth might deficits in

Development (2017) 144, 3102-3113 doi:10.1242/dev.145854

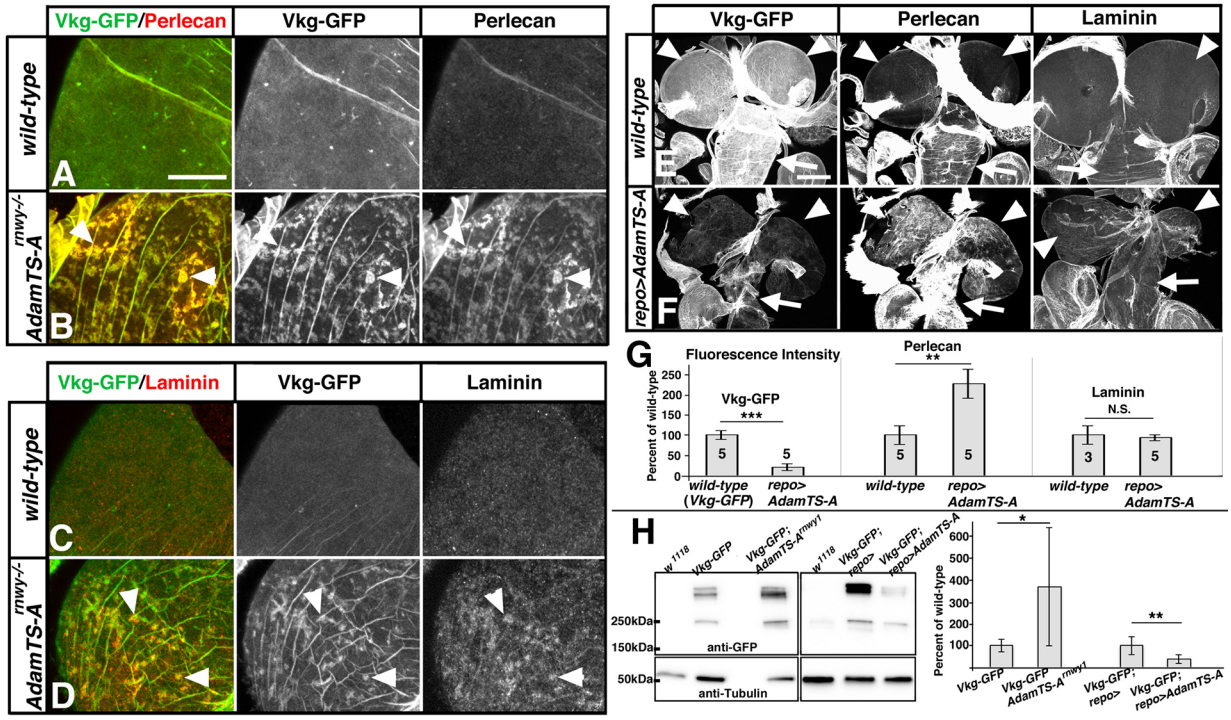

Fig. 7. *AdamTS-A* regulates the subcellular distribution of Viking-GFP, Perlecan and Laminin. (A-D) High-magnification views of the upper lateral region of a single brain lobe from late third instar wild-type (A,C) and *AdamTS-A*^{rnwy} mutant (B,D) larvae co-labeled for Viking-GFP and Perlecan (A,B) or Viking-GFP and Laminin (C,D). Arrowheads indicate aggregates or accumulations of Viking-GFP, Perlecan and Laminin localization in *AdamTS-A*$^{rnwy1/1}$ mutant larvae. Scale bar: 20 µm. (E,F) Ventral views of brain and ventral nerve cord labeled for Viking-GFP, Perlecan and Laminin in wild-type larvae and larvae overexpressing *AdamTS-A [RB]* in glia. Arrowheads indicate brain lobes; arrows indicate ventral nerve cord. Scale bar: 100 µm. (G) Quantification of fluorescence intensity in the brain of Vkg-GFP, Perlecan and Laminin in wild-type larvae (*vkg-GFP*) and *AdamTS-A[RB]* overexpression larvae. Numbers in the box refer to the number of animals analyzed; error bars indicate s.d. The levels of Viking-GFP are significantly decreased (***P<1×10^{-6}) and those of Perlecan increased (**P<0.0005) (Student's *t*-test). (H) Western blot of anti-GFP in the CNS of *vkg-GFP* and *vkg-GFP*; *AdamTS-A*^{rnwy1} larvae, as well as *vkg-GFP; repo>* and *vkg-GFP; repo>AdamTS-A* larvae. Right: quantification of western blots showing that Vkg-GFP levels are significantly increased in *AdamTS-A*^{rnwy} larvae (n=7; *P<0.05, *t*-test) and decreased in *repo>AdamTS-A* overexpressing larvae (n=6; **P<0.01); error bars indicate s.d. For more details of the full genotypes, see the supplementary Materials and Methods.

basement membrane function become manifest. For example, if *AdamTS-A* is required for the basement membrane to breathe and expand to keep pace with the growth of the CNS, reduction of *AdamTS-A* function might specifically inhibit basement membrane growth. Such a result might increase tissue tension on the growing CNS, perhaps indirectly triggering the mass exodus of neural lineages out of the CNS and the associated mass distortion of CNS structure.

Do AdamTS genes play conserved roles to anchor neural lineages in place?

Superficially, the *AdamTS-A*^{rnwy} phenotype resembles the phenomenon of perineural invasion, a major mode of metastasis, particularly in head and neck cancers, in which cancer cells migrate along or through nerves to distant sites (Liebig et al., 2009). This similarity hints that reduction of *AdamTS* function in mammalian glial cells may, in some contexts, contribute to perineural invasion and other modes of cancer spread. In support of this idea, like surface glia in flies, the glia limitans in mammals, a thin layer of astrocytic cellular processes overlain by the parencyhmal basement membrane, serves as the outermost layer of the CNS, fully enwrapping the CNS and spinal cord (Liu et al., 2013). In addition, *AdamTS-1*, *AdamTS-4*, *AdamTS-5* and *AdamTS-9*, the mammalian genes most closely related to *AdamTS-A*, are expressed in astrocytes and glia, but not in neurons, in the mammalian CNS (Demircan et al., 2013; Tauchi et al., 2012). And, in humans reduction in the expression of *AdamTS-9* has been associated with breast, pancreatic, colorectal and gastric cancer (Porter et al., 2004; Zhang et al., 2010), and specifically with cancer metastasis in nasopharyngeal cancer, a head and neck cancer (Lung et al., 2008). Clearly, it will be critical to determine whether *AdamTS* gene function is relevant to perineural invasion in humans and whether from flies to humans the *AdamTS* genes play conserved roles in the outermost cells of the CNS to preserve CNS structure and anchor neural lineages in place.

MATERIALS AND METHODS

Mutagenesis

A standard autosomal recessive forward genetic screen was carried out using 30 µm EMS to mutagenize a *P{w+}FRT2A P{neo+}FRT82B* isogenic chromosome. Homozygous mutant late-third instar larvae were manually dissected and scored for defects in CNS morphology.

Generation of *UAS-AdamTS-A[RB]* transgenic fly line

The UAS-linked *AdamTS-A[RB]* wild-type transgene was generated by amplifying region 905-5971 of the *AdamTS-A* cDNA, GH16393 (accession number AY094716). During PCR amplification, the 21-nucleotide sequence for Syn21, a translational enhancer effective in *Drosophila* (Pfeiffer et al., 2012), was added to the 5′ primer immediately upstream of the ATG start codon. The resulting PCR product was then cloned directionally into the *Kpn*I and *Xba*I sites of pJFRC28 (Pfeiffer et al., 2012) using Gibson Assembly Cloning Kit (New England Biolabs). Germline integrants of *the UAS-AdamTS-A[RB]* construct were then

Development (2017) 144, 3102-3113 doi:10.1242/dev.145854

generated via phi-C31-mediated cassette exchange into the *P{CaryP}attp2* site in the third chromosome (Rainbow Transgenic Flies). The UAS-linked *AdamTS-A[RB]* (*AdamTS-A^{E591A}*) protease-dead transgene was generated in an essentially identical manner and inserted into the same third chromosomal *P{CaryP}attp2* site.

Fly strains and standard genetic approaches

Fly strains used for meiotic mapping

For meiotic mapping, (i) *P{w[+]}BG00690*, (ii) *P{w[+]}Alh[BG02270]*, (iii) *P{w[+]}cher[BG02734]* and (iv) *P{w[+]}BG01881* strains were used.

Fly strains used for complementation crosses and deficiency mapping

For complementation crosses and deficiency mapping, *TM3 Sb^{1}*, *TM6C Sb^{1}*, *Gla Sb^{1}*, *Sb^{spi}*, *Sb^{2563}*, *Sb^{sbd-2}*, *Sb^{63b}*, *Df(3R)BSC750*, *Df(3R)ED5664*, *Df (3R)BSC741*, *Df(3R)Exel6174*, *Df(3R)BSC515*, *Df(3R)BSC569*, *Df(3R) 88F5* (Ismat et al., 2013), *AdamTS-A^{K0}* (Ismat et al., 2013) and *AdamTS-A^{MB04384}* strains were used.

GAL4-UAS experiments

To restrict UAS-linked transgene expression specifically to glia, we used the *repoGAL4* driver line. To restrict UAS-linked transgene expression specifically to neurons, we used a fly strain that carried both the *elavGAL4* driver line, which drives high level gene expression in neurons and lower level expression in glia, with *repoGAL80*, which blocks GAL4-mediated gene activation in glia. To drive UAS-linked transgenes ubiquitously, we used the *tubP-GAL4* driver line.

In the GAL4/UAS experiments that drove UAS-linked transgenes for *AdamTS-A*, we used two wild-type and two protease-dead *AdamTS-A* transgenes: in each case, one transgene encoded for the *AdamTS-A[RB]* transcript, which is specifically disrupted in the *AdamTS-A^{rnwy}* alleles and is predicted to produce a protein that contains an N-terminally, membrane-anchored protein, and the other transgene encoded for the *AdamTS-A[RE]* transcript (Ismat et al., 2013), which is predicted to produce a protein that lacks a membrane domain. The two wild-type transgenes and the two protease-dead transgenes behaved essentially identically in the noted assays. The *n* values provided for each experiment are the minimum number of samples assayed for each transgene.

GAL4 lines

The GAL4 lines used the study were: (i) *repoGAL4 UAS-CD8-GFP/TM6 Tb*, (ii) *repoGAL4 UAS-CD8-GFP AdamTS-A^{rnwy2}/TM6B Tb*, (iii) *repoGAL80/CyO-Dfd-GFP; elavGALl4* (Awasaki et al., 2008; Lin and Goodman, 1994), (iv) *repoGAL80/CyO-Dfd-GFP; elavGAL4 AdamTS-A^{rnwy2}/TM6B Tb*, (iv) *NP577GAL4* (specific for cortex glia; Hayashi et al., 2002), (v) *NP577GAL4; AdamTS-A^{rnwy1}/TM6B Tb*, (vi) *RL82-GAL4* (specific for subperineural glia; Sepp and Auld, 1999), (vii) *RL82-GAL4; AdamTS-A^{rnwy1}/TM6B Tb*, (viii) *SPG-GAL4* (specific for sub-perineural glia; Silies et al., 2007), (ix) *SPG-GAL4; AdamTS-A^{rnwy1}/TM6B Tb*, (x) *NP6293-GAL4* (specific for perineural glia; Hayashi et al., 2002), (xi) *NP6293-GAL4; AdamTS-A^{rnwy1}/TM6B Tb*, (xii) *mZ0709-GAL4* (specific for ensheathing glia; Ito et al., 1995), (xiii) *mZ0709-GAL4 AdamTS-A^{rnwy2}/TM6B Tb*, (xiv) *ALRM-GAL4* (specific for astrocyte-like glia; Doherty et al., 2009), (xv) *ALRM-GAL4*; *AdamTS-A^{rnwy1}/TM6B Tb*, (xvi) *tubP-GAL4/TM6 Tb* (Lee and Luo, 1999) and (xvii) *ppl-GAL4* (Colombani et al., 2003).

UAS-linked transgenes

UAS-linked transgenes used in the study were: (i) *UAS-AdamTS-A[RB]* (this paper) and *UAS-AdamTS-A[*RE] (Ismat et al., 2013), (ii) *UAS-AdamTS-A^{E591A}* (Transcript RB; this paper) and *UAS-AdamTS-A^{E439A}* (Transcript RE; Ismat et al., 2013), (iii) *UAS-AdamTS-A^{RNAi} (TRiP. HMJ21762); UAS-DCR2/TM6B Tb*, (iv) *UAS-AdamTS-A^{RNAi}* (*VDRC. KK.110157*), (v) *UAS-AdamTS-A^{WT}; Df(3R)88F5/TM6B Tb*, (vi) *UAS-AdamTS-A^{E439A}; Df(3R)88F5/TM6B Tb*, (vii) *UAS-NLS-GFP* (BSC#4775), (viii) *UAS-Ras^{DN} (UAS-Ras^{N17}; BSC#4846); AdamTS-A^{rnwy1}/TM6B Tb*, (ix) *UAS-Raf^{DN}* (de Celis, 1997); *AdamTS-A^{rnwy1}/TM6B Tb*, (x) *UAS-mys^{RNAi} (TRiP.JF02819) AdamTS-A^{rnwy1}/TM6B Tb*, (xi) *UAS-mys^{RNAi} (TRiP.HMS00043) AdamTS-A^{rnwy1}/TM6B Tb*, (xii) *UAS-trol^{RNAi}* (*TRiP. JF03376*), (xiii) *UAS-perlecan[RG]* (Cho et al., 2012) and (xiv) UAS-*viking^{RNAi}* (TRiP.HMC02400).

Additional lines used in the study were: (i) *trol^{G0271}/FM7-GFP*, (ii) *trol^{8}/FM7-GFP*, (iii) *trol^{SD}/FM7-GFP*, (iv) *Laminin A^{MI06740} AdamTS-A^{rnwy1}/TM6B Tb*, (v) *Df(2L)BSC172/CyO dfd-GFP; AdamTS-A^{rnwy1}/TM6B Tb*, (vi) *viking^{G00454}* (*viking-GFP*), (vii) *viking^{G07914}* (viking-GFP); *AdamTS-A^{rnwy1}/TM6B Tb*, (viii) *shg^{R69}/CyO dfd-GFP; AdamTS-A^{rnwy1}/TM6B Tb*, (ix) *Dg^{B48}/CyO dfd-GFP; AdamTS-A^{rnwy1}/TM6B Tb* and (x) *sdc^{K10215}/CyO dfd-GFP; AdamTS-A^{rnwy1}/TM6B Tb.*

We identified a second allele of *runaway* carried in the *TM3 Sb^{1}*, *TM6C Sb^{1}* and *Gla Sb^{1}* chromosomes, but not in chromosomes that harbored *Sb^{spi}*, *Sb^{2563}*, *Sb^{sbd-2}* or *Sb^{63b}*. *runaway^{2}* is likely *l(3)89Aa* (Nelson and Szauter, 1992) and was independently identified as an *AdamTS-A* allele by Ismat et al. (2013).

AdamTS-A^{GAL4} lines were generated from *AdamTS-A^{MI09007}* and *AdamTS-AMI^{14156}* (Nagarkar-Jaiswal et al., 2015) using the TROJAN-GAL4 system (Diao et al., 2015), following the cross scheme as detailed by Diao et al. (2015), except that *TM6 Tb* was used in place of *TM3 Sb* due to the presence of the *AdamTS-A^{rnwy2}* allele in the *TM3 Sb* chromosome.

Time to pupation and survival analyses

Flies of appropriate genotypes, e.g. *AdamTS-A^{rnwy1}/TM6B Tb* × *Df(3R) 88F5/TM6B Tb*, were allowed to lay eggs for 12 h in vials. Vials were checked daily for *Tb* and *non-Tb* pupae and adults. Expected number of *non-Tb* pupae and adults was calculated as one-half observed number of *Tb* pupae or adults.

Antibody generation and immunofluoresence studies

DNA encoding amino acids 78-431 of Deadpan was cloned into pET29a (Novagen) for protein expression and purification. Protein-specific antibody responses were mounted in guinea pigs (Pocono Rabbit Farm and Laboratory, PA, USA) and the resulting sera was used at a 1:500-1:1000 dilution. The resulting anti-sera specifically recognize neuroblasts in the embryonic and larval CNS.

The following antibodies and molecular probes were used in this study: rabbit anti-GFP (1:1000, Torrey Pines Biolabs), mouse monoclonal antibody 9F8A9 (ELAV; 1:20) and rat monoclonal antibody 7E8A10 (ELAV; 1:100) (O'Neill et al., 1994), mouse monoclonal antibody 8D12 (REPO; 1:100) (Alfonso and Jones, 2002), rabbit anti-Laminin (1:1000) (Fessler et al., 1987), rabbit anti-Perlecan (1:1000) (Friedrich et al., 2000), goat anti-HRP-Cy5 (1:1000; Jackson Labs) and DAPI (1:1000; Calbiochem). Gene expression analyses were performed as described by Patel (1994), using the noted antibodies and molecular probes. All imaging was performed on a Zeiss LSM-700 Confocal Microscope and Zen software.

When protein expression levels were compared between genotypes (e.g. for Viking-GFP, Perlecan and Laminin), brain-imaginal disc complexes were dissected at the same time, fixed and stained in the same tube, mounted on the same slide and imaged sequentially using identical parameters on a Zeiss LSM 700 Confocal microscope.

Sequencing

Genomic DNA was obtained from *P{w+}FRT2A P{neo+}FRT82B* larvae or larvae homozygous or hemizygous mutant, respectively, for *AdamTS-A^{rnwy1}* or *AdamTS-A^{rnwy2}* and provided to GENEWIZ or GTAC (Washington University) for Sanger or next-generation sequencing.

qRT-PCR analysis

The following protocol was carried out in triplicate for each genotype. Approximately 80-100 CNS-imaginal disc complexes from wild-type (*P{w+}FRT2A P{neo+}FRT82B*) or *AdamTS-A^{rnwy1}* were dissected on ice and then immediately homogenized in TRIzol reagent (Life Technologies). RNA was extracted following standard protocols, treated with DNase I, and then quantified. For each qRT PCR reaction, 500 ng of total RNA was reverse transcribed using random primers (Promega) and the SMARTScribe Reverse Transcriptase (Clontech). qRT-PCR was then performed on *rp49* as an internal control and the *AdamTS-A[RB]* transcript. The *AdamTS-A*

Development (2017) 144, 3102-3113 doi:10.1242/dev.145854

primers flanked the ~25 kb first intron of the largest and main AdamTS-A [RB] transcript. Two technical replicates and no-RT controls were performed for each RNA sample for each genotype. rp49 primers were 5′-CCGCTTCAAGGGACAGTATCTG and 3′-ATCTCGCCGCAGTAA-ACGC; and *AdamTS-A* primers were 5′-CTGCGGTATTCGCTGAAAG-GAC and 3′-CGATGCAGCAGGCATACAGG.

Acknowledgements

We thank Drs Swathi Arur, Heather Broihier and Andrea Page-McCaw for critical comments on the manuscript. We thank Drs Deborah Andrews, Afshan Ismat, Marc Freeman, Stefan Baumgartner, Steve Johnson, Andrea Page-McCaw, Tim Schedl and Craig Micchelli for fly lines and reagents. We thank the Iowa Developmental Studies Hybridoma Bank for antibodies, and Kathy Matthews, Kevin Cook and the Bloomington Stock Center for countless fly lines.

Competing interests

The authors declare no competing or financial interests.

Author contributions

Conceptualization: J.B.S., H.L.; Methodology: J.B.S., B.A.W., S.E.R., M.J.S., Y.Z., H.L.; Validation: J.B.S.; Formal analysis: J.B.S., S.E.R., M.J.S., Y.Z., H.L.; Investigation: J.B.S., B.A.W., S.E.R., M.J.S., Y.Z.; Resources: J.B.S.; Data curation: J.B.S., Y.Z.; Writing - original draft: J.B.S.; Writing - review & editing: J.B.S.; Visualization: J.B.S., H.L.; Supervision: J.B.S.; Project administration: J.B.S., B.A.W.; Funding acquisition: J.B.S.

Funding

This work was supported by grants from the National Institutes of Health (NS036570) and the McDonnell Center for Cellular and Molecular Neurobiology to J.B.S. S.E.R. was a fellow in the National Human Genome Research Institute-funded Opportunities for Genomic Research Program (R25HG006687). Deposited in PMC for release after 12 months.

Supplementary information

Supplementary information available online at
http://dev.biologists.org/lookup/doi/10.1242/dev.145854.supplemental

References

Alfonso, T. B. and Jones, B. W. (2002). gcm2 promotes glial cell differentiation and is required with glial cells missing for macrophage development in Drosophila. *Dev. Biol.* **248**, 369-383.

Apte, S. S. (2009). A disintegrin-like and metalloprotease (reprolysin-type) with thrombospondin type 1 motif (ADAMTS) superfamily: functions and mechanisms. *J. Biol. Chem.* **284**, 31493-31497.

Awasaki, T., Lai, S.-L., Ito, K. and Lee, T. (2008). Organization and postembryonic development of glial cells in the adult central brain of Drosophila. *J. Neurosci.* **28**, 13742-13753.

Bainton, R. J., Tsai, L. T.-Y., Schwabe, T., DeSalvo, M., Gaul, U. and Heberlein, U. (2005). moody encodes two GPCRs that regulate cocaine behaviors and blood-brain barrier permeability in Drosophila. *Cell* **123**, 145-156.

Berger, C., Renner, S., Lüer, K. and Technau, G. M. (2007). The commonly used marker ELAV is transiently expressed in neuroblasts and glial cells in the Drosophila embryonic CNS. *Dev. Dyn.* **236**, 3562-3568.

Blelloch, R. and Kimble, J. (1999). Control of organ shape by a secreted metalloprotease in the nematode Caenorhabditis elegans. *Nature* **399**, 586-590.

Brand, A. H. and Perrimon, N. (1993). Targeted gene expression as a means of altering cell fates and generating dominant phenotypes. *Development* **118**, 401-415.

Burnside, E. R. and Bradbury, E. J. (2014). Review: manipulating the extracellular matrix and its role in brain and spinal cord plasticity and repair. *Neuropathol. Appl. Neurobiol.* **40**, 26-59.

Capy, P., Gasperi, G., Biémont, C. and Bazin, C. (2000). Stress and transposable elements: Co-evolution or useful parasites? *Heredity (Edinb).* **85**, 101-106.

Carlos Rodriguez-Manzaneque, J., Westling, J., Thai, S. N. M., Luque, A., Knauper, V., Murphy, G., Sandy, J. D. and Iruela-Arispea, M. L. (2002). ADAMTS1 cleaves aggrecan at multiple sites and is differentially inhibited by metalloproteinase inhibitorsq. *Biochem. Biophys. Res. Commun.* **293**, 501-508.

Cho, J. Y., Chak, K., Andreone, B. J., Wooley, J. R. and Kolodkin, A. L. (2012). The extracellular matrix proteoglycan perlecan facilitates transmembrane semaphorin-mediated repulsive guidance. *Genes Dev.* **26**, 2222-2235.

Colombani, J., Raisin, S., Pantalacci, S., Radimerski, T., Montagne, J. and Léopold, P. (2003). A nutrient sensor mechanism controls Drosophila growth. *Cell* **114**, 739-749.

Coutinho-Budd, J. and Freeman, M. R. (2013). Probing the enigma: Unraveling glial cell biology in invertebrates. *Curr. Opin. Neurobiol.* **23**, 1073-1079.

Crabbe, T., Zucker, S., Cockett, M. I., Willenbrock, F., Tickle, S., O'Connell, J. P., Scothern, J. M., Murphy, G. and Docherty, A. J. P. (1994). Mutation of the active site glutamic acid of human gelatinase A: effects on latency, catalysis, and the binding of tissue inhibitor of metalloproteinases-1. *Biochemistry* **33**, 6684-6690.

Datta, S. (1995). Control of proliferation activation in quiescent neuroblasts of the Drosophila central nervous system. *Development* **121**, 1173-1182.

Datta, S. and Kankel, D. R. (1992). l(1)trol and l(1)devl, loci affecting the development of the adult central nervous system in Drosophila melanogaster. *Genetics* **130**, 523-537.

de Celis, J. F. (1997). Expression and function of decapentaplegic and thick veins during the differentiation of the veins in the Drosophila wing. *Development* **124**, 1007-1018.

Demircan, K., Yonezawa, T., Takigawa, T., Topcu, V., Erdogan, S., Ucar, F., Armutcu, F., Yigitoglu, M. R., Ninomiya, Y. and Hirohata, S. (2013). ADAMTS1, ADAMTS5, ADAMTS9 and aggrecanase-generated proteoglycan fragments are induced following spinal cord injury in mouse. *Neurosci. Lett.* **544**, 25-30.

Diao, F., Ironfield, H., Luan, H., Diao, F., Shropshire, W. C., Ewer, J., Marr, E., Potter, C. J., Landgraf, M. and White, B. H. (2015). Plug-and-play genetic access to drosophila cell types using exchangeable exon cassettes. *Cell Rep.* **10**, 1410-1421.

Doherty, J., Logan, M. A., Taşdemir, O. E. and Freeman, M. R. (2009). Ensheathing glia function as phagocytes in the adult Drosophila brain. *J. Neurosci.* **29**, 4768-4781.

Fessler, L. I., Campbell, A. G., Duncan, K. G. and Fessler, J. H. (1987). Drosophila laminin: Characterization and localization. *J. Cell Biol.* **105**, 2383-2391.

Friedrich, M. V. K., Schneider, M., Timpl, R. and Baumgartner, S. (2000). Perlecan domain V of Drosophila melanogaster. Sequence, recombinant analysis and tissue expression. *Eur. J. Biochem.* **267**, 3149-3159.

Hayashi, S., Ito, K., Sado, Y., Taniguchi, M., Akimoto, A., Takeuchi, H., Aigaki, T., Matsuzaki, F., Nakagoshi, H., Tanimura, T. et al. (2002). GETDB, a database compiling expression patterns and molecular locations of a collection of Gal4 enhancer traps. *Genesis* **34**, 58-61.

Ismat, A., Cheshire, A. M. and Andrew, D. J. (2013). The secreted AdamTS-A metalloprotease is required for collective cell migration. *Development* **140**, 1981-1993.

Ito, K., Urban, J. and Technau, G. M. (1995). Distribution, classification, and development of Drosophila glial cells in the late embryonic and early larval ventral nerve cord. *Roux's Arch. Dev. Biol.* **204**, 284-307.

Kai, F. B., Laklai, H. and Weaver, V. M. (2016). Force matters: biomechanical regulation of cell invasion and migration in disease. *Trends Cell Biol.* **26**, 486-497.

Kelwick, R., Desanlis, I., Wheeler, G. N. and Edwards, D. R. (2015). The ADAMTS (A Disintegrin and Metalloproteinase with Thrombospondin motifs) family. *Genome Biol.* **16**, 113.

Kim, H.-S. and Nishiwaki, K. (2015). Control of the basement membrane and cell migration by ADAMTS proteinases: Lessons from C. elegans genetics. *Matrix Biol.* **44-46**, 64-69.

Kim, S. N., Jeibmann, A., Halama, K., Witte, H. T., Wälte, M., Matzat, T., Schillers, H., Faber, C., Senner, V., Paulus, W. et al. (2014). ECM stiffness regulates glial migration in Drosophila and mammalian glioma models. *Development* **141**, 3233-3242.

Kuno, K., Kanada, N., Nakashima, E., Fujiki, F., Ichimura, F. and Matsushima, K. (1997). Molecular cloning of a gene encoding a new type of metalloproteinase-disintegrin family protein with thrombospondin motifs as an inflammation associated gene. *J. Biol. Chem.* **272**, 556-562.

Lee, T. and Luo, L. (1999). Mosaic analysis with a repressible cell marker for studies of gene function in neuronal morphogenesis. *Neuron* **22**, 451-461.

Liebig, C., Ayala, G., Wilks, J., Verstovsek, G., Liu, H., Agarwal, N., Berger, D. H. and Albo, D. (2009). Perineural invasion is an independent predictor of outcome in colorectal cancer. *J. Clin. Oncol.* **27**, 5131-5137.

Lin, D. M. and Goodman, C. S. (1994). Ectopic and increased expression of Fasciclin II alters motoneuron growth cone guidance. *Neuron* **13**, 507-523.

Liu, X., Zhang, Z., Guo, W., Burnstock, G., He, C. and Xiang, Z. (2013). The superficial glia limitans of mouse and monkey brain and spinal cord. *Anat. Rec.* **296**, 995-1007.

Lo, C.-M., Wang, H.-B., Dembo, M. and Wang, Y. L. (2000). Cell movement is guided by the rigidity of the substrate. *Biophys. J.* **79**, 144-152.

Lung, H. L., Lo, P. H. Y., Xie, D., Apte, S. S., Cheung, A. K. L., Cheng, Y., Law, E. W. L., Chua, D., Zeng, Y.-X., Sai, W. T. et al. (2008). Characterization of a novel epigenetically-silenced, growth-suppressive gene, ADAMTS9, and its association with lymph node metastases in nasopharyngeal carcinoma. *Int. J. Cancer* **123**, 401-408.

Maurange, C., Cheng, L. and Gould, A. P. (2008). Temporal transcription factors and their targets schedule the end of neural proliferation in Drosophila. *Cell* **133**, 891-902.

Medjkane, S., Perez-Sanchez, C., Gaggioli, C., Sahai, E. and Treisman, R. (2009). Myocardin-related transcription factors and SRF are required for cytoskeletal dynamics and experimental metastasis. *Nat. Cell Biol.* **11**, 257-268.

Meyer, S., Schmidt, I., Klämbt, C. and Klämbt, C. (2014). Glia ECM interactions are required to shape the Drosophila nervous system. *Mech. Dev.* **3**, 105-116.

Morin, X., Daneman, R., Zavortink, M. and Chia, W. (2001). A protein trap strategy to detect GFP-tagged proteins expressed from their endogenous loci in Drosophila. *Proc. Natl. Acad. Sci. USA* **98**, 15050-15055.
Nagarkar-Jaiswal, S., Deluca, S. Z., Lee, P. T., Lin, W. W., Pan, H., Zuo, Z., Lv, J., Spradling, A. C. and Bellen, H. J. (2015). A genetic toolkit for tagging intronic MiMIC containing genes. *Elife* **4**, e08469.
Nelson, C. R. and Szauter, P. (1992). Cytogenetic analysis of chromosome region 89A of Drosophila melanogaster: Isolation of deficiencies and mapping of Po, Aldox-1 and transposon insertions. *Mol. Gen. Genet.* **235**, 11-21.
Nishiwaki, K., Hisamoto, N. and Matsumoto, K. (2000). A metalloprotease disintegrin that controls cell migration in Caenorhabditis elegans. *Science* **288**, 2205-2208.
O'Neill, E. M., Rebay, I., Tjian, R. and Rubin, G. M. (1994). The activities of two Ets-related transcription factors required for Drosophila eye development are modulated by the Ras/MAPK pathway. *Cell* **78**, 137-147.
Pastor-Pareja, J. C. and Xu, T. (2011). Shaping cells and organs in drosophila by opposing roles of fat body-secreted collagen IV and perlecan. *Dev. Cell* **21**, 245-256.
Patel, N. H. (1994). Imaging neuronal subsets and other cell types in whole-mount Drosophila embryos and larvae using antibody probes. *Methods Cell Biol.* **44**, 445-487.
Pfeiffer, B. D., Truman, J. W. and Rubin, G. M. (2012). Using translational enhancers to increase transgene expression in Drosophila. *Proc. Natl. Acad. Sci.* **109**, 6626-6631.
Porter, S., Scott, S. D., Sassoon, E. M., Williams, M. R., Jones, J. L., Girling, A. C., Ball, R. Y. and Edwards, D. R. (2004). Dysregulated expression of adamalysin-thrombospondin genes in human breast carcinoma. *Clin. Cancer Res.* **10**, 2429-2440.
Rodriguez-Manzaneque, J. C., Fernandez-Rodriguez, R., Rodriguez-Baena, F. J. and Iruela-Arispe, M. L. (2015). ADAMTS proteases in vascular biology. *Matrix Biol.* **44-46**, 38-45.
Sandy, J. D., Westling, J., Kenagy, R. D., Iruela-Arispe, M. L., Verscharen, C., Rodriguez-Mazaneque, J. C., Zimmermann, D. R., Lemire, J. M., Fischer, J. W., Wight, T. N. et al. (2001). Versican V1 proteolysis in human aorta in vivo occurs at the Glu 441-Ala442 bond, a site that is cleaved by recombinant ADAMTS-1 and ADAMTS-4. *J. Biol. Chem.* **276**, 13372-13378.
Sepp, K. J. and Auld, V. J. (1999). Conversion of lacZ enhancer trap lines to GAL4 lines using targeted transposition in Drosophila melanogaster. *Genetics* **151**, 1093-1101.
Silies, M., Yuva, Y., Engelen, D., Aho, A., Stork, T. and Klämbt, C. (2007). Glial cell migration in the eye disc. *J. Neurosci.* **27**, 13130-13139.
Somerville, R. P. T., Longpre, J.-M., Jungers, K. A., Engle, J. M., Ross, M., Evanko, S., Wight, T. N., Leduc, R. and Aptell, S. S. (2003). Characterization of ADAMTS-9 and ADAMTS-20 as a distinct ADAMTS subfamily related to Caenorhabditis elegans GON-1. *J. Biol. Chem.* **278**, 9503-9513.
Stork, T., Engelen, D., Krudewig, A., Silies, M., Bainton, R. J. and Klämbt, C. (2008). Organization and function of the blood-brain barrier in Drosophila. *J. Neurosci.* **28**, 587-597.
Tauchi, R., Imagama, S., Natori, T., Ohgomori, T., Muramoto, A., Shinjo, R., Matsuyama, Y., Ishiguro, N. and Kadomatsu, K. (2012). The endogenous proteoglycan-degrading enzyme ADAMTS-4 promotes functional recovery after spinal cord injury. *J. Neuroinflammation* **9**, 53.
Truman, J. W. and Bate, M. (1988). Spatial and temporal patterns of neurogenesis in the central nervous system of Drosophila melanogaster. *Dev. Biol.* **125**, 145-157.
Volkenhoff, A., Weiler, A., Letzel, M., Stehling, M., Klämbt, C. and Schirmeier, S. (2015). Glial glycolysis is essential for neuronal survival in drosophila. *Cell Metab.* **22**, 437-447.
Yurchenco, P. D. (2011). Basement membranes: cell scaffoldings and signaling platforms. *Cold Spring Harb. Perspect. Biol.* **3**, a004911.
Zhai, R. G., Hiesinger, P. R., Koh, T.-W., Verstreken, P., Schulze, K. L., Cao, Y., Jafar-Nejad, H., Norga, K. K., Pan, H., Bayat, V. et al. (2003). Mapping Drosophila mutations with molecularly defined P element insertions. *Proc. Natl. Acad. Sci. USA* **100**, 10860-10865.
Zhang, C., Shao, Y., Zhang, W., Wu, Q., Yang, H., Zhong, Q., Zhang, J., Guan, M., Yu, B. and Wan, J. (2010). High-resolution melting analysis of ADAMTS9 methylation levels in gastric, colorectal, and pancreatic cancers. *Cancer Genet. Cytogenet.* **196**, 38-44.
Zimmer, G., Schanuel, S. M., Bürger, S., Weth, F., Steinecke, A., Bolz, J. and Lent, R. (2010). Chondroitin sulfate acts in concert with semaphorin 3A to guide tangential migration of cortical interneurons in the ventral telencephalon. *Cereb. Cortex* **20**, 2411-2422.